The Astronomical Journal, 142:115 (9pp), 2011 October doi:10.1088/0004-6256/142/4/115

TERMS PHOTOMETRY OF KNOWN TRANSITING EXOPLANETS

Diana Dragomir[1,2], Stephen R. Kane[1], Genady Pilyavsky[3], Suvrath Mahadevan[3,4], David R. Ciardi[1], J. Zachary Gazak[5], Dawn M. Gelino[1], Alan Payne[1], Markus Rabus[6], Solange V. Ramirez[1], Kaspar von Braun[1], Jason T. Wright[3,4], and Pamela Wyatt[1]
[1] NASA Exoplanet Science Institute, Caltech, MS 100-22, Pasadena, CA 91125, USA
[2] Department of Physics & Astronomy, University of British Columbia, Vancouver, BC V6T1Z1, Canada; diana@phas.ubc.ca
[3] Department of Astronomy and Astrophysics, Pennsylvania State University, University Park, PA 16802, USA
[4] Center for Exoplanets & Habitable Worlds, Pennsylvania State University, University Park, PA 16802, USA
[5] Institute for Astronomy, University of Hawaii, Honolulu, HI 96822, USA
[6] Departamento de Astronomía y Astrofísica, Pontificia Universidad Católica de Chile, Casilla 306, Santiago 22, Chile
Received 2011 May 3; accepted 2011 July 29; published 2011 September 8

ABSTRACT

The Transit Ephemeris Refinement and Monitoring Survey conducts radial velocity and photometric monitoring of known exoplanets in order to refine planetary orbits and predictions of possible transit times. This effort is primarily directed toward planets not known to transit, but a small sample of our targets consists of known transiting systems. Here we present precision photometry for six WASP (Wide Angle Search for Planets) planets acquired during their transit windows. We perform a Markov Chain Monte Carlo analysis for each planet and combine these data with previous measurements to redetermine the period and ephemerides for these planets. These observations provide recent mid-transit times which are useful for scheduling future observations. Our results improve the ephemerides of WASP-4b, WASP-5b, and WASP-6b and reduce the uncertainties on the mid-transit time for WASP-29b. We also confirm the orbital, stellar, and planetary parameters of all six systems.

Key words: planetary systems – stars: individual (WASP-4, WASP-5, WASP-6, WASP-19, WASP-29, WASP-31) – techniques: photometric

Online-only material: color figures

1. INTRODUCTION

Over 100 transiting planets have now been discovered and confirmed, and the *Kepler* mission has contributed over 1200 additional candidates (Borucki et al. 2011). Transit observations provide a wealth of information about a planet's physical properties. The majority of known transiting exoplanets have arisen from ground-based surveys such as SuperWASP (Pollacco et al. 2006), HATNet (Bakos et al. 2004), TrES (O'Donovan et al. 2006), and XO (McCullough et al. 2005).

The majority of these planets are hot Jupiters and are anything but standardized compared to each other with respect to their density and orbital parameters. In particular, several inflated hot Jupiters have been discovered (such as HD 209458 b, first detected by Charbonneau et al. 2000), with large radii relative to their masses. One explanation for this effect is tidal heating, which has been shown to inflate the radii of close-in planets even when the orbital eccentricity is very small (Bodenheimer et al. 2001; Miller et al. 2009). Other proposed mechanisms include enhanced atmospheric opacities (Burrows et al. 2007) and ohmic dissipation (Batygin & Stevenson 2010), but none seem to be able to account for the entire sample of inflated hot Jupiters.

The Transit Ephemeris Refinement and Monitoring Survey (TERMS) is a project which aims to refine the orbital parameters of intermediate-long period radial velocity planets and detect their transits (Kane et al. 2009). We present photometry for six of the WASP planets. These data were acquired in order to demonstrate the precision we can achieve for these and other TERMS targets in general with the Cerro Tololo Inter-American Observatory (CTIO) 1.0 m telescope, and to test the data reduction pipeline. All six are gas giants, with WASP-4b, WASP-5b, WASP-6b, and WASP-6b orbiting G-type stars while WASP-29b orbits a K dwarf and WASP-31b orbits an F star. The six host stars have apparent magnitudes in the range $11.3 < m_V < 12.6$. Each system is interesting in its own right. WASP-4b (Wilson et al. 2008), WASP-6b (Gillon et al. 2009a), and WASP-31b (Anderson et al. 2011) are low-density, inflated planets. Possible indications of transit timing variations (TTVs; Agol et al. 2005) have been reported for WASP-5b (Gillon et al. 2009b; Fukui et al. 2011) since its discovery (Anderson et al. 2008). WASP-19b (Hebb et al. 2010) has the shortest period of all the known hot Jupiters, and is thus extremely interesting from a dynamical point of view. WASP-29b (Hellier et al. 2010) is one of only a handful of Saturn-mass (and radius) planets.

In this paper we independently derive parameters for these planets and their host stars, and provide updated ephemerides for each system based on the observed transits.

In Section 2, we describe the photometric observations and their reduction. The analysis of these data and the results are presented in Sections 3 and 4, respectively. We summarize and discuss the results in Section 5.

2. OBSERVATIONS AND DATA REDUCTION

The observations[7] were carried out at CTIO, with most of the data acquired using the 1.0 m telescope and the Y4KCam CCD detector. The field of view of this instrument is $20' \times 20'$ and the readout time of the detector is 51 s. The earlier of two light curves for WASP-4 was obtained using the 0.9 m telescope, which has a CCD with a $13'.5 \times 13'.5$ field of view and a readout time of 53 s.

[7] The photometry presented in this paper will be made publicly available through the NASA Star and Exoplanet Database (NStED) at http://nsted.ipac.caltech.edu.

Table 1
Log of Observations

WASP Exoplanet	Date	Telescope	Filter	Exp. Time (s)	No. of Exposures	σ_{red}[a] (Rel. Flux)	σ^{a}_{white} (Rel. Flux)	rms (Rel. Flux)
WASP-4b	2008 Oct 12	CTIO 0.9 m	*V*	60	165	0.0110	0.0021	0.0029
WASP-4b	2009 Sep 10	CTIO 1.0 m	*R*	150	80	0.0139	0.0011	0.0026
WASP-5b	2009 Aug 31	CTIO 1.0 m	*R*	300	36	0.00262	0.00033	0.0007
WASP-5b	2010 Sep 8	CTIO 1.0 m	*R*	90	109	0.0046	0.0011	0.0013
WASP-6b	2010 Sep 6	CTIO 1.0 m	*R*	120	101	0.00691	0.00056	0.0013
WASP-19b	2011 Jan 18	CTIO 1.0 m	*R*	90	127	0.0073	0.0010	0.0013
WASP-29b	2010 Sep 5	CTIO 1.0 m	*R*	30	185	0.00450	0.00089	0.0012
WASP-31b	2011 Jan 25	CTIO 1.0 m	*R*	90	87	0.0063	0.0011	0.0017

Notes. [a] σ_{red} is the red noise parameter and σ_{white} is the white noise parameter. The values for each were obtained using TAP. It is important to note that even though σ_{white} is the rms of the white noise, σ_{red} is not the rms of the red noise (Carter & Winn 2009).

WASP-4 was observed on the night of 2008 October 12, using a Johnson *V*-band filter, and the night of 2009 September 10 with a Cousins *R*-band filter. The remaining five WASP targets were observed through a Cousins *R*-band filter.

The photometry for WASP-5 was obtained on the nights of 2009 August 31 and of 2010 September 8.

The photometry for WASP-6 was obtained on the night of 2010 September 6. The photometry for WASP-19 was obtained on the night of 2011 January 18. WASP-29 was observed on the night of 2010 September 5. WASP-31 was observed on the night of 2011 January 25. Detailed information pertaining to the observations can be found in Table 1.

All images were bias subtracted and flat-fielded using skyflats. To increase the signal-to-noise ratio per pixel and prevent individual pixel counts from exceeding the linear response range of the CCD, we defocussed the images to produce a relatively large point-spread function (PSF), similar to that described by Southworth et al. (2009b). The excellent guiding capabilities of the telescope allowed the stellar profile to remain on or near the same pixels such that accurate aperture photometry was able to be performed. Aperture radii that corresponded to the extent of the PSF and sky annuli chosen so as not to include any nearby stars were used for the photometry. We found that the photometry is relatively robust against the choice of these aperture radii. Between two and four carefully selected reference stars were used in each case. Reference stars were generally fainter than the target. Brighter stars were often saturated (the 0.9 m and the 1.0 m CCDs are linear up ~40,000 ADU above bias) because exposure times were optimized to obtain maximum flux for the target while maintaining the peak counts of the PSF within the linear regime of the CCD. Relative photometry was performed using the methods described in Everett & Howell (2001).

After performing aperture photometry on the transit of WASP-6b, a trend was still visible in the light curve. The trend correlates with airmass and is likely due to different spectral types of the reference stars relative to the target. Since the algorithm we used to fit the light curves (see Section 3) can only perform a linear correction for the airmass, we removed it by fitting a second-order polynomial to the out-of-transit data (using time as the independent parameter) and subtracting it from the entire light curve.

3. ANALYSIS

We used the Transit Analysis Package (TAP) developed by Gazak et al. (2011) to obtain stellar and planetary parameters from our new light curves. TAP accepts single or multiple light curves as input. The light curves are then fitted using the Mandel & Agol (2002) model by means of a Markov Chain Monte Carlo (MCMC) analysis. In the case of multiple transits, the parameters for each transit can either evolve together or independently. This allows us, for example, to fit the transit midpoint of each transit separately while a single value is obtained for each of the remaining fitted parameters. We ran TAP with the eccentricity (e) and the argument of periastron (ω) fixed to previously published values because these parameters are generally more accurately determined by radial velocity measurements, and because it is difficult to constrain their values using only one or two transits for each target.

The planet-to-star radius ratio (R_P/R_*), the scaled semimajor axis (a/R_*), the inclination (i), and the time of mid-transit (T_0) were allowed to float. The period was fixed to the most recent published value (as of 2011 May) for each planet. We have also allowed the algorithm to fit for two additional parameters: uncorrelated (white) noise and correlated (red) noise. TAP uses a wavelet likelihood function to more robustly estimate parameter uncertainties, particularly in cases where the light curve is affected by correlated noise (Carter & Winn 2009). For each WASP light curve, we ran 10 chains of 10^6 steps each, and removed the initial 10% of each chain to account for burn-in.

We have analyzed all of our data with fixed limb darkening coefficients (assuming a quadratic limb darkening law), using values interpolated from the tables of Claret (2000) appropriate for each star. We have also repeated the analysis with u_1 and u_2 as free parameters. Since those two parameters are correlated, the uncorrelated linear combinations $2u_1 + u_2$ and $u_1 - 2u_2$ were fitted instead (Holman et al. 2006). For all six systems, the values of the parameters obtained when the limb darkening coefficients were allowed to float are only slightly different than those obtained by fixing the limb darkening coefficients, and they agree within uncertainties. In all cases, the fitted values of u_1 and u_2 had large uncertainties (~±0.3 for u_1 and ~±0.4 for u_2), indicating that our photometry does not improve upon the known limb darkening properties of these stars. These values were consistent with the Claret (2000) values within uncertainties.

Hence the parameter values we report have been obtained by fixing the values of the limb darkening coefficients, except for one of the WASP-4b analyses.

While we acquired one transit each for WASP-6b, WASP-19b, WASP-29b, and WASP-31b, we observed and analyzed two transits each for WASP-4b and WASP-5b. For WASP-4b, we have analyzed the light curves separately since they were taken using different filters. However, we have also performed a combined analysis of the two data sets in order to obtain

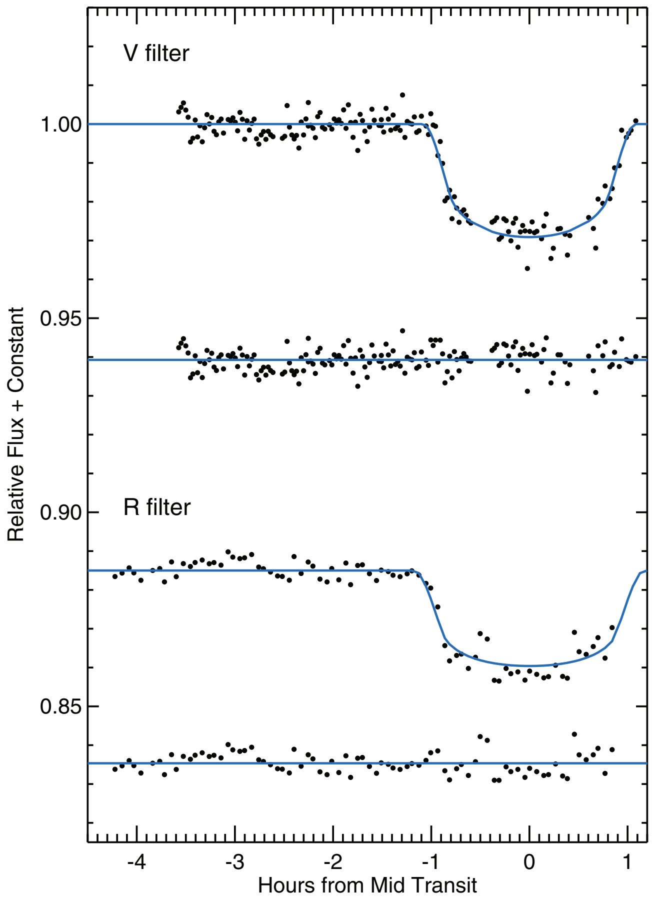

Figure 1. CTIO 0.9 m *V*-band (top) and 1.0 m *R*-band (bottom) transit photometry of WASP-4b. The blue line is the best-fit transit light curve. The residuals are shown below each transit (rms = 2900 ppm for the *V*-band transit, and rms = 2600 ppm for the *R*-band transit). See Tables 3 and 4 for the WASP-4 system parameters.

(A color version of this figure is available in the online journal.)

more accurate and precise estimates of the stellar and planetary parameters. In this case we allowed the limb darkening coefficients to float, since fixing them is inappropriate due to the different filters. For completeness, we report the results of all three analyses of the WASP-4b light curves (Tables 3 and 4). In the case of WASP-5b, we have analyzed both light curves together and derived a single value for each transit parameter except the mid-transit time (for which we obtained one value per transit).

Our transit light curves for the six planets are shown in Figures 1 to 6, respectively.

4. RESULTS

4.1. New Mid-transit Times and Ephemerides

Since their discovery, new transit times have been published for both of WASP-4b and WASP-5b (Gillon et al. 2009b; Southworth et al. 2009a, 2009b; Triaud et al. 2010; Fukui et al. 2011). This wealth of data naturally invites TTV analyses. However, we believe that for such an analysis to be consistent and as accurate as possible, all available transit photometry for a given system should be fitted using the same algorithm and the results analyzed using the same method. This is beyond the scope of this paper, but we encourage such studies which are now becoming increasingly possible with the advent of online exoplanet databases such as the NASA Star and Exoplanet Database (von Braun et al. 2009).

For the purpose of this paper, we combine the mid-transit times from our analysis with all previously published times to maximize the time span of observations, and use them to determine a new ephemeris for each system. For each of

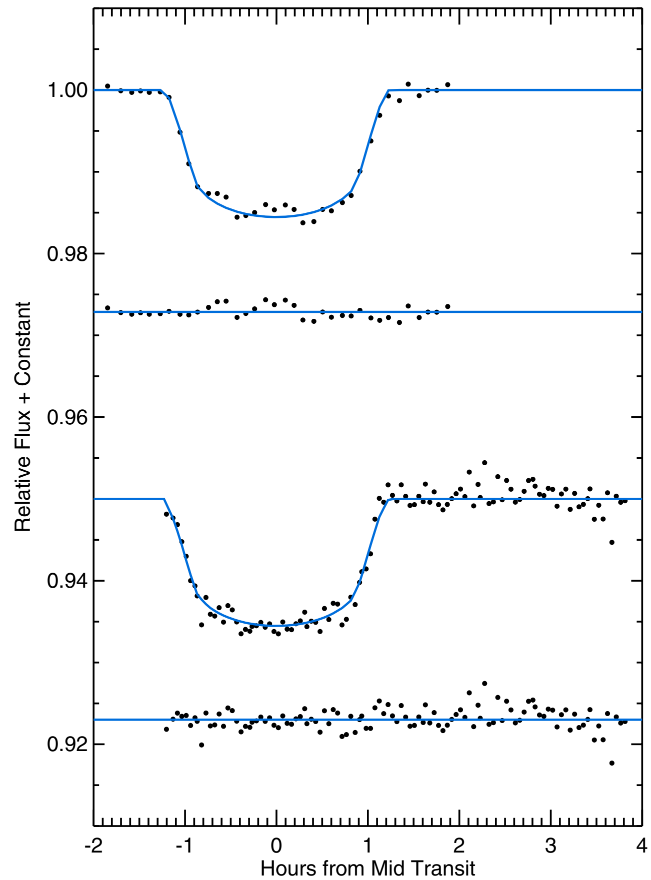

Figure 2. CTIO 1.0 m *R*-band (bottom) transit photometry of WASP-5b, observed on 2009 August 31 (top) and 2010 September 8 (bottom). The blue line is the best-fit transit light curve. The residuals are shown below each transit (rms = 700 ppm for the top transit, and rms = 1300 ppm for the bottom transit). See Table 5 for the WASP-5 system parameters.

(A color version of this figure is available in the online journal.)

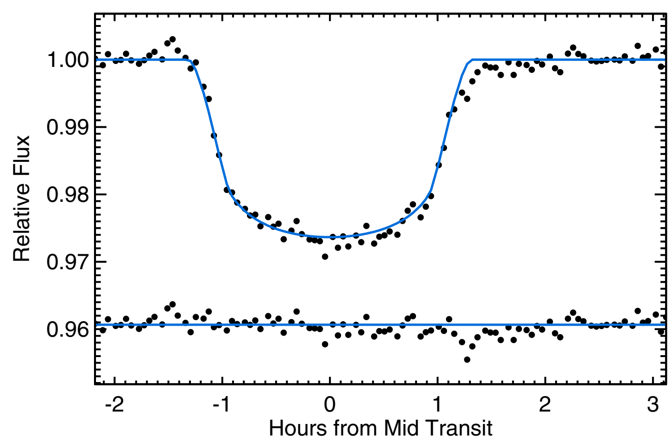

Figure 3. CTIO 1.0 m *R*-band transit photometry of WASP-6b, after airmass correction (see the text for details). The blue line is the best-fit transit light curve. The residuals are shown at the bottom of the figure (rms = 1300 ppm). See Table 6 for the WASP-6 system parameters.

(A color version of this figure is available in the online journal.)

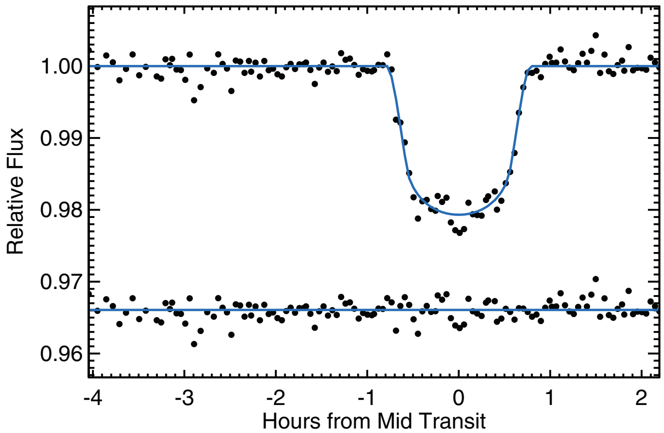

Figure 4. CTIO 1.0 m *R*-band transit photometry of WASP-19b. The blue line is the best-fit transit light curve. The residuals are shown at the bottom of the figure (rms = 1300 ppm). See Table 7 for the WASP-19 system parameters.

(A color version of this figure is available in the online journal.)

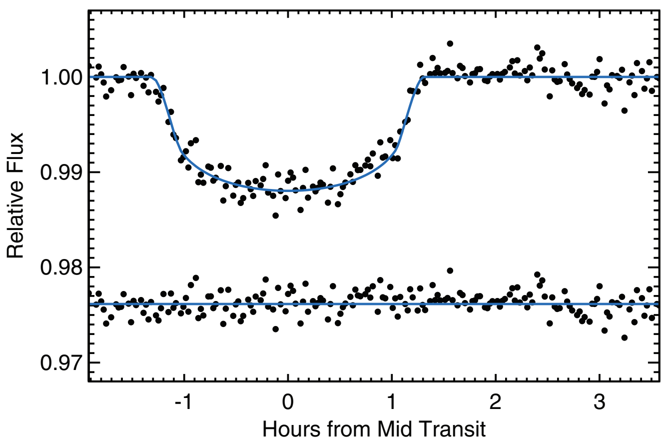

Figure 5. CTIO 1.0 m *R*-band transit photometry of WASP-29b. The blue line is the best-fit transit light curve. The residuals are shown at the bottom of the figure (rms = 1200 ppm). See Table 8 for the WASP-29 system parameters.

(A color version of this figure is available in the online journal.)

WASP-4b and WASP-5b we have acquired and analyzed two transits. The two transits were observed about one year apart for each target. Together with the 15 published values for WASP-4b (Gillon et al. 2009b; Winn et al. 2009; Southworth et al. 2009a; Sanchis-Ojeda et al. 2011) we have a total of 17 mid-transit points. For WASP-5b, we combined 13 published values (Gillon et al. 2009b; Southworth et al. 2009b; Fukui et al. 2011) with our two for a total of 15 mid-transit points.

For WASP-19b, we used three mid-transit times: two previously published values (Hebb et al. 2010; Hellier et al. 2011) and the one corresponding to the transit we have observed. Hellier et al. (2011) did not report the mid-transit time corresponding to the transit they obtained on the night of 2010 February 28 because they performed a combined analysis of both that transit and the one presented in Hebb et al. (2010). We fitted the data obtained by C. Hellier et al. (2011, private communication) using TAP (as described in Section 3) to obtain the mid-transit time.

For each of WASP-6b, WASP-29b, and WASP-31b, we have one transit which we combined with the original published values (Gillon et al. 2009a, Hellier et al. 2010, and Anderson et al. 2011, respectively) for a total of two mid-transit points for each system.

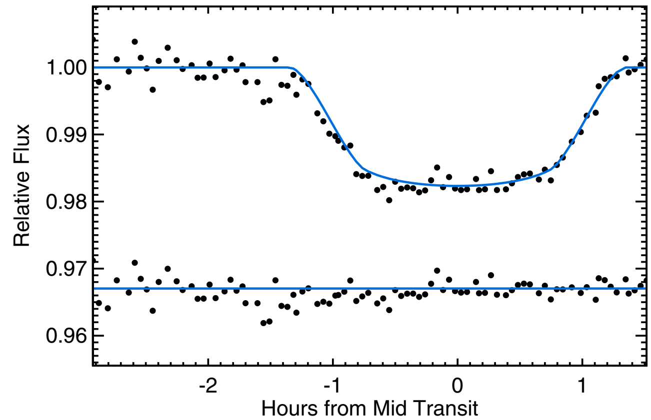

Figure 6. CTIO 1.0 m *R*-band transit photometry of WASP-31b. The blue line is the best-fit transit light curve. The residuals are shown at the bottom of the figure (rms = 1700 ppm). See Table 9 for the WASP-31 system parameters.

(A color version of this figure is available in the online journal.)

When necessary, these times were converted from $\mathrm{JD_{UTC}}$ (our values) and from $\mathrm{HJD_{UTC}}$ (the discovery paper values) to $\mathrm{BJD_{TDB}}$ using the online calculator developed by Eastman et al. (2010). We determined a new ephemeris by fitting a linear function to the mid-transit points for each system:

$$T_0[n] = T_0[0] + nP. \quad (1)$$

We chose to center the set of mid-transit times we used for each exoplanet so as to minimize the covariance between $T_0[0]$ and P. This means that the values of T_0 reported in Tables 3–9 do not necessarily correspond to any of the mid-transit times in Table 2 for a specific planet. The covariance calculated in this manner is sufficiently small for its influence in the calculation of the uncertainty on future mid-transit times to be negligible.

4.2. Determination of Stellar and Planetary Properties

For each system, the values of the orbital eccentricity, argument of periastron, velocity semi-amplitude (K), stellar mass (M_*), and planet mass (M_P) were taken from previous publications (see footnotes of Tables 3–9 for details). These values together with the light curve parameters were used to calculate the remaining parameters in the tables. Two of those quantities, the stellar density (ρ_*) and the planet surface gravity (g_P), can be obtained solely from the photometry. For ρ_* we used the equation

$$\rho_* + k^3 \rho_P = \frac{3\pi}{GP^2}\left(\frac{a}{R_*}\right)^3 \quad (2)$$

from Seager & Mallén-Ornelas (2003), where k is a constant coefficient for each stellar sequence, which relates the stellar mass and radius, ρ_P is the planetary density, and P is the orbital period. Since k^3 is usually small (Winn 2010), Equation (2) becomes

$$\rho_* \approx \frac{3\pi}{GP^2}\left(\frac{a}{R_*}\right)^3. \quad (3)$$

We calculated g_P using

$$g_P = \frac{2\pi}{P}\frac{\sqrt{1-e^2}K_*}{(R_P/a)^2 \sin i}, \quad (4)$$

which is derived in Southworth et al. (2007).

In Tables 3–9 we report our parameter estimates for the stellar and planetary properties.

Table 2
Mid-transit Times for All Six WASP Exoplanets

WASP Exoplanet	Epoch	Mid-transit Time (BJD_{TDB})	Filter	Reference
	−549	$2453963.10863^{+0.00074}_{-0.00081}$	*R*	Gillon et al. (2009b)[a]
	−249	$2454364.57722^{+0.00068}_{-0.00075}$	*R*	Gillon et al. (2009b)[a]
	−246	$2454368.59244^{+0.00022}_{-0.00019}$	*R*	Gillon et al. (2009b)
	−244	$2454371.26812^{+0.00033}_{-0.00028}$	*I*	Gillon et al. (2009b)
	−225	$2454396.695410^{0.000051+}_{-0.000051}$	*Z*	Gillon et al. (2009b)
	0	$2454697.797489^{+0.000055}_{-0.000055}$	*Z*	Winn et al. (2009)
	0	$2454697.798219^{+0.00010}_{-0.00010}$	*R*	Southworth et al. (2009a)
	3	$2454701.812919^{+0.00013}_{-0.00013}$	*R*	Southworth et al. (2009a)
WASP-4b	26	$2454732.591919^{0.00013+}_{-0.00013}$	*R*	Southworth et al. (2009a)
	32	$2454740.621560^{0.000061+}_{-0.000061}$	*R*	Southworth et al. (2009a)
	38	$2454748.650490^{0.000072+}_{-0.000072}$	*Z*	Winn et al. (2009)
	41	$2454752.66591^{+0.00071}_{-0.00071}$	*V*	This work
	260	$2455045.738643^{+0.000054}_{-0.000054}$	*Z*	Sanchis-Ojeda et al. (2011)
	263	$2455049.753274^{+0.000066}_{-0.000066}$	*Z*	Sanchis-Ojeda et al. (2011)
	266	$2455053.767816^{+0.000053}_{-0.000053}$	*Z*	Sanchis-Ojeda et al. (2011)
	290	$2455085.8853^{+0.0038}_{-0.0016}$	*R*	This work
	301	$2455100.605928^{+0.000061}_{-0.000061}$	*Z*	Sanchis-Ojeda et al. (2011)
	−264	$2453945.71962^{+0.00091}_{-0.00093}$	*R*	Gillon et al. (2009b)[a]
	−7	$2454364.2283^{+0.0012}_{-0.0013}$	*R*	Gillon et al. (2009b)[a]
	5	$2454383.76751^{0.00028+}_{-0.00028}$	*R*	Gillon et al. (2009b)
	7	$2454387.02286^{0.00086+}_{-0.00086}$	*I*	Gillon et al. (2009b)
	160	$2454636.17465^{+0.00047}_{-0.00047}$	*I*	Fukui et al. (2011)
	204	$2454707.82531^{+0.00021}_{-0.00021}$	*R*	Southworth et al. (2009b)
	218	$2454730.62252^{+0.00022}_{-0.00022}$	*R*	Southworth et al. (2009b)
WASP-5b	244	$2454772.96212^{+0.00051}_{-0.00051}$	*I*	Fukui et al. (2011)
	430	$2455075.84936^{+0.00055}_{-0.00056}$	*R*	This work
	432	$2455079.10849^{+0.00044}_{-0.00044}$	*I*	Fukui et al. (2011)
	451	$2455110.04645^{+0.00073}_{-0.00073}$	*I*	Fukui et al. (2011)
	459	$2455123.07627^{+0.00041}_{-0.00041}$	*I*	Fukui et al. (2011)
	607	$2455364.08262^{+0.00057}_{-0.00057}$	*I*	Fukui et al. (2011)
	615	$2455377.10969^{+0.00048}_{-0.00048}$	*I*	Fukui et al. (2011)
	659	$2455448.75950^{+0.00086}_{-0.00084}$	*R*	This work
WASP-6b	0	$2454596.43342^{+0.00015}_{-0.00010}$	...	Gillon et al. (2009a)[a]
	253	$2455446.76621^{+0.00058}_{-0.00057}$	*R*	This work
	0	$2454775.33796^{+0.00010}_{-0.00020}$	...	Hebb et al. (2010)[a]
WASP-19b	609	$2455255.74105^{+0.00014}_{-0.00015}$	*R*	C. Hellier et al. (2011, private communication)
	1021	$2455580.74124^{+0.00057}_{-0.00059}$	*R*	This work
WASP-29b	0	$2455320.2348^{+0.0040}_{-0.0040}$	...	Hellier et al. (2010)[a]
	32	$2455445.76247^{+0.00073}_{-0.00070}$	*R*	This work
WASP-31b	0	$2455189.2836^{+0.0003}_{-0.0003}$	...	Anderson et al. (2011)[a]
	117	$2455587.7719^{+0.0014}_{-0.0013}$	*R*	This work

Note. [a] The mid-transit times reported in the discovery papers for these targets were computed based on several transits.

5. DISCUSSION

We present new photometry for six known transiting exoplanet systems: WASP-4, WASP-5, WASP-6, WASP-19, WASP-29, and WASP-31. We have reduced the data and used TAP—an interactive MCMC-based software package—to fit the transit photometry. The code robustly evaluates parameter uncertainties using a wavelet-based method for dealing with red noise in the light curves and fits for white and red noise, as well as any linear trend that may be present in the data (due to airmass, for example), in addition to the transit parameters. Based on the photometry and radial velocity-derived parameters obtained from the literature, we compute and report new values for the orbital parameters, as well as the stellar and planetary properties of these six systems. Specifically, we determine the mid-transit time, the scaled semimajor axis, the planet/star area ratio, and the orbital inclination solely from our new photometric measurements. The values for the orbital eccentricity, the

Table 3
System Parameters for WASP-4 (*V* and *R* Light Curves Analyzed Separately)

Parameter	Symbol	This Work (*V* Filter)	This Work (*R* Filter)
Mid-transit time (BJD_{TDB})	T_0	$2454823.591767^{+0.000019}_{-0.000019}$	$2454823.591767^{+0.000019}_{-0.000019}$
Orbital period (days)	P	$1.33823326^{+0.00000011}_{-0.00000011}$	$1.33823326^{+0.00000011}_{-0.00000011}$
Scaled semimajor axis	a/R_*	$5.45^{+0.15}_{-0.24}$	$4.96^{+0.38}_{-0.62}$
Planet/star area ratio	$(R_p/R_*)^2$	$0.0233^{+0.0017}_{-0.0015}$	$0.0205^{+0.0030}_{-0.0030}$
Orbital inclination (deg)	i	$88.2^{+1.2}_{-1.9}$	$87.2^{+2.0}_{-2.9}$
Transit duration[a] (hr)	t_T	$2.154^{+0.083}_{-0.114}$	$2.32^{+0.19}_{-0.30}$
Semimajor axis (AU)	a	$0.02320^{+0.00042}_{-0.00042}$	$0.02320^{+0.00042}_{-0.00042}$
Orbital eccentricity	e	0 (adopted)	0 (adopted)
Argument of periastron (deg)	ω	...	...
Velocity semi-amplitude (m s^{-1})	K	$242.1^{+2.8}_{-3.1}$ (adopted)	$242.1^{+2.8}_{-3.1}$ (adopted)
Stellar mass ($M_\odot$)	M_*	$0.93^{+0.05}_{-0.05}$ (adopted)	$0.93^{+0.05}_{-0.05}$ (adopted)
Stellar radius ($R_\odot$)	R_*	$0.915^{+0.030}_{-0.043}$	$1.005^{+0.079}_{-0.127}$
Stellar density (g cm^{-3})	ρ_*	$1.71^{+0.19}_{-0.26}$	$1.29^{+0.31}_{-0.49}$
Stellar surface gravity (cgs)	$\log g_*$	$4.484^{+0.037}_{-0.047}$	$4.402^{+0.072}_{-0.112}$
Planet mass (M_{Jup})	M_P	$1.250^{+0.050}_{-0.051}$ (adopted)	$1.250^{+0.050}_{-0.051}$ (adopted)
Planet radius (R_{Jup})	R_P	$1.389^{+0.068}_{-0.080}$	$1.43^{+0.15}_{-0.21}$
Planet density (g cm^{-3})	ρ_P	$0.619^{+0.095}_{-0.110}$	$0.56^{+0.18}_{-0.25}$
Planet surface gravity (cgs)	$\log g_P$	$3.225^{+0.046}_{-0.050}$	$3.199^{+0.093}_{-0.125}$

Notes. [a] The transit duration is from first contact to fourth contact. Uncertainties correspond to the 68.3% (1σ) confidence limits. The orbital eccentricity, argument of periastron, velocity semi-amplitude, stellar mass, and planet mass for WASP-4 were taken from Triaud et al. (2010).

Table 4
System Parameters for WASP-4 (*V* and *R* Light Curves Analyzed Together)

Parameter	Symbol	This Work (Combined)	Triaud et al. (2010)
Mid-transit time (BJD_{TDB})	T_0	$2454823.591767^{+0.000019}_{-0.000019}$	$2454387.327787^{+0.000040}_{-0.000039}$
Orbital period (days)	P	$1.33823326^{+0.00000011}_{-0.00000011}$	$1.3382299^{+0.0000023}_{-0.0000021}$
Scaled semimajor axis	a/R_*	$5.53^{+0.16}_{-0.21}$	$5.5313^{+0.011}_{-0.012}$
Planet/star area ratio	$(R_p/R_*)^2$	$0.0230485^{+0.0016}_{-0.0017}$.	$0.023333^{+0.000043}_{-0.000073}$
Orbital inclination (deg)	i	$88.5^{+1.0}_{-1.6}$	$89.47^{+0.51}_{-0.24}$
Transit duration[a] (hr)	t_T	$2.128^{+0.080}_{-0.096}$	$2.1283^{+0.0019}_{-0.0003}$
Semimajor axis (AU)	a	$0.02320^{+0.00042}_{-0.00042}$	$0.02320^{+0.00044}_{-0.00045}$
Orbital eccentricity	e	0 (adopted)	<0.0182
Argument of periastron (deg)	ω	...	...
Velocity semi-amplitude (m s^{-1})	K	$242.1^{+2.8}_{-3.1}$ (adopted)	$242.1^{+2.8}_{-3.1}$
Stellar mass ($M_\odot$)	M_*	$0.93^{+0.05}_{-0.05}$ (adopted)	$0.93^{+0.05}_{-0.05}$
Stellar radius ($R_\odot$)	R_*	$0.902^{+0.031}_{-0.038}$	$0.903^{+0.016}_{-0.019}$
Stellar density (g cm^{-3})	ρ_*	$1.79{+}0.21_{-0.24}$	$1.786^{+0.012}_{-0.011}$
Stellar surface gravity (cgs)	$\log g_*$	$4.496^{+0.038}_{-0.043}$	$4.5^{+0.2}_{-0.2}$
Planet mass (M_{Jup})	M_P	$1.250^{+0.050}_{-0.051}$ (adopted)	$1.250^{+0.050}_{-0.051}$
Planet radius (R_{Jup})	R_P	$1.363^{+0.066}_{-0.076}$	$1.341^{+0.023}_{-0.029}$
Planet density (g cm^{-3})	ρ_P	$0.655^{+0.098}_{-0.112}$	...
Planet surface gravity (cgs)	$\log g_P$	$3.242^{+0.045}_{-0.048}$	...

Notes. [a] The transit duration is from first contact to fourth contact. Uncertainties correspond to the 68.3% (1σ) confidence limits. The orbital eccentricity, argument of periastron, velocity semi-amplitude, stellar mass, and planet mass for WASP-4 were taken from Triaud et al. (2010).

argument of periastron, the velocity semi-amplitude, and the stellar and planetary masses are adopted from the literature (as described in the footnotes of Tables 3–9). The transit duration, the semimajor axis, as well as the stellar and planetary radii, densities and surface gravities were calculated from combinations of light curve parameters and parameters adopted from the literature. This work also constitutes the first follow-up observation paper for WASP-6b, WASP-29b, and WASP-31b since publication of the discovery papers.

All our parameter values—except the period—for the WASP-4, WASP-6, and WASP-31 systems agree with those published by Triaud et al. (2010), Gillon et al. (2009a), and

Table 5
System Parameters for WASP-5

Parameter	Symbol	This Work	Fukui et al. (2011)
Mid-transit time (BJD$_{\rm TDB}$)	T_0	$2454782.73290^{+0.00010}_{-0.00010}$	$2454375.62510^{+0.00019}_{-0.00019}$
Orbital period (days)	P	$1.62843064^{+0.00000057}_{-0.00000057}$	$1.62843142^{+0.00000064}_{-0.00000064}$
Scaled semimajor axis	a/R_*	$4.78^{+0.30}_{-0.23}$	$5.37^{+0.15}_{-0.15}$
Planet/star area ratio	$(R_p/R_*)^2$	$0.01392^{+0.00066}_{-0.00070}$	$0.01228^{+0.00024}_{-0.00024}$
Orbital inclination (deg)	i	$83.0^{+1.4}_{-1.1}$	$85.58^{+0.81}_{-0.76}$
Transit duration[a] (hr)	t_T	$2.49^{+0.29}_{-0.23}$	...
Semimajor axis (AU)	a	$0.02709^{+0.00057}_{-0.00058}$	$0.02702^{+0.00059}_{-0.00059}$
Orbital eccentricity	e	0 (adopted)	...
Argument of periastron (deg)	ω	...	...
Velocity semi-amplitude (m s^{-1})	K	$268.7^{+1.8}_{-1.9}$ (adopted)	...
Stellar mass ($M_\odot$)	M_*	$1.000^{+0.063}_{-0.064}$ (adopted)	...
Stellar radius ($R_\odot$)	R_*	$1.218^{+0.081}_{-0.064}$	$1.082^{+0.038}_{-0.038}$
Stellar density (g cm^{-3})	ρ_*	$0.78^{+0.16}_{-0.13}$	$1.11^{+0.14}_{-0.14}$
Stellar surface gravity (cgs)	$\log g_*$	$4.267^{+0.064}_{-0.053}$	
Planet mass ($M_{\rm Jup}$)	M_P	$1.555^{+0.066}_{-0.072}$ (adopted)	$1.568^{+0.071}_{-0.071}$
Planet radius ($R_{\rm Jup}$)	R_P	$1.430^{+0.100}_{-0.083}$	$1.167^{+0.043}_{-0.043}$
Planet density (g cm^{-3})	ρ_P	$0.71^{+0.15}_{-0.13}$	$1.22^{+0.15}_{-0.15}$
Planet surface gravity (cgs)	$\log g_P$	$3.298^{+0.064}_{-0.051}$	...

Notes. [a] The transit duration is from first contact to fourth contact. Uncertainties correspond to the 68.3% (1σ) confidence limits. The orbital eccentricity, argument of periastron, velocity semi-amplitude, stellar mass, and planet mass for WASP-5 were taken from Triaud et al. (2010).

Table 6
System Parameters for WASP-6

Parameter	Symbol	This Work	Gillon et al. (2009a)
Mid-transit time (BJD$_{\rm TDB}$)	T_0	$2454633.40441^{+0.00012}_{-0.00012}$	$2454596.43341^{+0.00015}_{-0.00010}$
Orbital period (days)	P	$3.3609992^{+0.0000023}_{-0.0000023}$	$3.3610060^{+0.0000022}_{-0.0000035}$
Scaled semimajor axis	a/R_*	$10.18^{+0.62}_{-0.80}$	...
Planet/star area ratio	$(R_p/R_*)^2$	$0.0223^{+0.0013}_{-0.0012}$	$0.02092^{+0.00019}_{-0.00025}$
Orbital inclination (deg)	i	$87.9^{+1.3}_{-1.1}$	$88.47^{+0.65}_{-0.47}$
Transit duration[a] (hr)	t_T	$2.75^{+0.27}_{-0.30}$	$2.606^{+0.018}_{-0.016}$
Semimajor axis (AU)	a	$0.04208^{+0.00080}_{-0.00128}$	$0.0421^{+0.0008}_{-0.0013}$
Orbital eccentricity	e	$0.054^{+0.018}_{-0.017}$ (adopted)	$0.054^{+0.018}_{-0.017}$
Argument of periastron (deg)	ω	$97.4^{+6.9}_{-13.2}$ (adopted)	$97.4^{+6.9}_{-13.2}$
Velocity semi-amplitude (m s^{-1})	K	$74.3^{+1.7}_{-1.4}$ (adopted)	$74.3^{+1.7}_{-1.4}$
Stellar mass ($M_\odot$)	M_*	$0.880^{+0.050}_{-0.080}$ (adopted)	$0.880^{+0.050}_{-0.080}$
Stellar radius ($R_\odot$)	R_*	$0.889^{+0.057}_{-0.075}$	$0.870^{+0.025}_{-0.036}$
Stellar density (g cm^{-3})	ρ_*	$1.77^{+0.35}_{-0.47}$	$1.89^{+0.16}_{-0.14}$
Stellar surface gravity (cgs)	$\log g_*$	$4.485^{+0.061}_{-0.083}$	$4.50^{+0.06}_{-0.06}$
Planet mass ($M_{\rm Jup}$)	M_P	$0.503^{+0.019}_{-0.038}$ (adopted)	$0.503^{+0.019}_{-0.038}$
Planet radius ($R_{\rm Jup}$)	R_P	$1.321^{+0.092}_{-0.12}$	$1.224^{+0.051}_{-0.052}$
Planet density (g cm^{-3})	ρ_P	$0.289^{+0.062}_{-0.080}$	$0.36^{+0.07}_{-0.07}$
Planet surface gravity (cgs)	$\log g_P$	$2.873^{+0.064}_{-0.077}$	$2.940^{+0.063}_{-0.063}$

Notes. [a] The transit duration is from first contact to fourth contact. Uncertainties correspond to the 68.3% (1σ) confidence limits. The orbital eccentricity, argument of periastron, velocity semi-amplitude, stellar mass, and planet mass for WASP-6 were taken from Gillon et al. (2009a).

Anderson et al. (2011), respectively, within the 1σ uncertainties, while the period agrees within the 2σ uncertainties in each case.

The parameter values stemming from the combined analysis of the WASP-4 light curves (Table 4) agree better with the results of Triaud et al. (2010) and are more precise than the parameter values based on the individual V-band and R-band light curves (Table 3).

All of our results for the WASP-29 system agree with those reported by Hellier et al. (2010) within the 1σ uncertainties, and our uncertainties on the mid-transit time are smaller. The estimates of the planetary radius are of comparable precision,

Table 7
System Parameters for WASP-19

Parameter	Symbol	This Work	Hellier et al. (2011)
Mid-transit time (BJD_{TDB})	T_0	$2455041.96557^{+0.00010}_{-0.00010}$	$2455168.96879^{+0.00009}_{-0.00009}$
Orbital period (days)	P	$0.78883889^{+0.00000032}_{-0.00000032}$	$0.7888400^{+0.0000003}_{-0.0000003}$
Scaled semimajor axis	a/R_*	$4.02^{+0.39}_{-0.38}$	...
Planet/star area ratio	$(R_p/R_*)^2$	$0.0180^{+0.0014}_{-0.0013}$	$0.0206^{+0.0002}_{-0.0002}$
Orbital inclination (deg)	i	$83.0^{+3.8}_{-2.8}$	$79.4^{+0.4}_{-0.4}$
Transit duration[a] (hr)	t_T	$1.55^{+0.26}_{-0.23}$	$1.572^{+0.007}_{-0.007}$
Semimajor axis (AU)	a	$0.01654^{+0.00011}_{-0.00011}$	$0.01655^{+0.00013}_{-0.00013}$
Orbital eccentricity	e	0 (adopted)	$0.0046^{+0.0044}_{-0.0028}$
Argument of periastron (deg)	ω	...	3^{+70}_{-70}
Velocity semi-amplitude (m s^{-1})	K	257^{+3}_{-3} (adopted)	257^{+3}_{-3}
Stellar mass ($M_{\odot}$)	M_*	$0.97^{+0.02}_{-0.02}$ (adopted)	$0.97^{+0.02}_{-0.02}$
Stellar radius ($R_{\odot}$)	R_*	$0.885^{+0.086}_{-0.084}$	$0.99^{+0.02}_{-0.02}$
Stellar density (g cm^{-3})	ρ_*	$1.98^{+0.59}_{-0.58}$	$1.400^{+0.066}_{-0.059}$
Stellar surface gravity (cgs)	$\log g_*$	$4.531^{+0.085}_{-0.083}$	$4.432^{+0.013}_{-0.013}$
Planet mass (M_{Jup})	M_P	$1.168^{+0.023}_{-0.023}$ (adopted)	$1.168^{+0.023}_{-0.023}$
Planet radius (R_{Jup})	R_P	$1.18^{+0.12}_{-0.12}$	$1.386^{+0.032}_{-0.032}$
Planet density (g cm^{-3})	ρ_P	$0.94^{+0.29}_{-0.28}$	$0.581^{+0.037}_{-0.037}$
Planet surface gravity (cgs)	$\log g_P$	$3.330^{+0.091}_{-0.088}$	$3.143^{+0.018}_{-0.018}$

Notes. [a] The transit duration is from first contact to fourth contact. Uncertainties correspond to the 68.3% (1σ) confidence limits. The orbital eccentricity, velocity semi-amplitude, stellar mass, and planet mass for WASP-19 were taken from Hellier et al. (2011).

Table 8
System Parameters for WASP-29

Parameter	Symbol	This Work	Hellier et al. (2010)
Mid-transit time (BJD_{TDB})	T_0	$2455441.83973^{+0.00070}_{-0.00070}$	$2455320.2348^{+0.0040}_{-0.0040}$
Orbital period (days)	P	$3.92274^{+0.00013}_{-0.00013}$	$3.922727^{+0.000004}_{-0.000004}$
Scaled semimajor axis	a/R_*	$11.98^{+0.69}_{-1.25}$	...
Planet/star area ratio	$(R_p/R_*)^2$	$0.00977^{+0.00079}_{-0.00061}$	$0.0102^{+0.0004}_{-0.0004}$
Inclination (deg)	i	$88.3^{+1.1}_{-1.2}$	$88.8^{+0.7}_{-0.7}$
Transit duration[a] (hr)	t_T	$2.60^{+0.25}_{-0.36}$	$2.659^{+0.036}_{-0.036}$
Semimajor axis (AU)	a	$0.04566^{+0.00061}_{-0.00061}$	$0.0457^{+0.0006}_{-0.0006}$
Eccentricity	e	0 (adopted)	$0.03^{+0.05}_{-0.03}$
Argument of periastron (deg)	ω	...	...
Velocity semi-amplitude (m s^{-1})	K	$35.6^{+2.7}_{-2.7}$ (adopted)	$35.6^{+2.7}_{-2.7}$
Stellar mass ($M_{\odot}$)	M_*	$0.825^{+0.033}_{-0.033}$ (adopted)	$0.825^{+0.033}_{-0.033}$
Stellar radius ($R_{\odot}$)	R_*	$0.820^{+0.048}_{-0.086}$	$0.808^{+0.044}_{-0.044}$
Stellar density (g cm^{-3})	ρ_*	$2.11^{+0.38}_{-0.67}$	$2.20^{+0.28}_{-0.32}$
Stellar surface gravity (cgs)	$\log g_*$	$4.527^{+0.054}_{-0.093}$	$4.54^{+0.04}_{-0.04}$
Planet mass (M_{Jup})	M_P	$0.244^{+0.020}_{-0.020}$ (adopted)	$0.244^{+0.020}_{-0.020}$
Planet radius (R_{Jup})	R_P	$0.806^{+0.058}_{-0.089}$	$0.792^{+0.056}_{-0.035}$
Planet density (g cm^{-3})	ρ_P	$0.61^{+0.14}_{-0.21}$	$0.65^{+0.11}_{-0.11}$
Planet surface gravity (cgs)	$\log g_P$	$2.987^{+0.071}_{-0.101}$	$2.95^{+0.05}_{-0.05}$

Notes. [a] The transit duration is from first contact to fourth contact. Uncertainties correspond to the 68.3% (1σ) confidence limits. The orbital eccentricity, argument of periastron, velocity semi-amplitude, stellar mass, and planet mass for WASP-29 were taken from Hellier et al. (2010).

confirming its Saturn-like size. For the WASP-19 system, our values for all parameters agree with those reported by Hellier et al. (2011) within the 2σ uncertainties. Our value for the stellar radius of WASP-5 agrees with the value reported by (Fukui et al. 2011, hereafter F10) within the 2σ uncertainties, which in turn causes our value for the planet radius to be about 23% larger than that reported in the same paper. The remaining stellar and planetary parameters agree within the 2σ uncertainties. F10 analyzed seven new transits together with all previously published transit photometry for this system, and detected a deviation from a linear ephemeris which, if real, corresponds to TTVs with amplitudes of up to 50 s. They also find a period which does not agree with previously published values within error bars, which can be considered as a possible indication of

Table 9
System Parameters for WASP-31

Parameter	Symbol	This Work	Anderson et al. (2011)
Mid-transit time (BJD$_{TDB}$)	T_0	$2455209.71890^{+0.00029}_{-0.00029}$	$2455189.2836^{+0.0003}_{-0.0003}$
Orbital period (days)	P	$3.40588291^{+0.000012}_{-0.000012}$	$3.405909^{+0.000005}_{-0.000005}$
Scaled semimajor axis	a/R_*	$8.52^{+1.04}_{-0.81}$	...
Planet/star area ratio	$(R_p/R_*)^2$	$0.0171^{+0.0016}_{-0.0015}$	$0.01622^{+0.00032}_{-0.00032}$
Inclination (deg)	i	$85.17^{+1.09}_{-0.93}$	$84.54^{+0.27}_{-0.27}$
Transit duration[a] (hr)	t_T	$2.67^{+0.64}_{-0.52}$	$2.657^{+0.034}_{-0.034}$
Semimajor axis (AU)	a	$0.04657^{+0.00035}_{-0.00035}$	$0.04657^{+0.00034}_{-0.00034}$
Eccentricity	e	0 (adopted)	0 (adopted)
Argument of periastron (deg)	ω	...	...
Velocity semi-amplitude (m s^{-1})	K	$58.2^{+3.5}_{-3.5}$ (adopted)	$58.2^{+3.5}_{-3.5}$
Stellar mass ($M_\odot$)	M_*	$1.161^{+0.026}_{-0.026}$ (adopted)	$1.161^{+0.026}_{-0.026}$
Stellar radius ($R_\odot$)	R_*	$1.18^{+0.14}_{-0.11}$	$1.241^{+0.039}_{-0.039}$
Stellar density (g cm^{-3})	ρ_*	$1.01^{+0.37}_{-0.29}$	$0.857^{+0.073}_{-0.073}$
Stellar surface gravity (cgs)	$\log g_*$	$4.363^{+0.107}_{-0.083}$	$4.316^{+0.024}_{-0.024}$
Planet mass (M_{Jup})	M_P	$0.478^{+0.030}_{-0.030}$ (adopted)	$0.478^{+0.030}_{-0.030}$
Planet radius (R_{Jup})	R_P	$1.53^{+0.20}_{-0.16}$	$1.537^{+0.060}_{-0.060}$
Planet density (g cm^{-3})	ρ_P	$0.177^{+0.070}_{-0.057}$	$0.175^{+0.023}_{-0.023}$
Planet surface gravity (cgs)	$\log g_P$	$2.724^{+0.117}_{-0.095}$	$2.665^{+0.042}_{-0.042}$

Notes. [a] The transit duration is from first contact to fourth contact. Uncertainties correspond to the 68.3% (1σ) confidence limits. The orbital eccentricity, argument of periastron, velocity semi-amplitude, stellar mass, and planet mass for WASP-31 were taken from Anderson et al. (2011).

TTVs as well. Our period value for WASP-5b is consistent with that determined by F10 within the 1σ uncertainties, but, like theirs, differs from those obtained by Southworth et al. (2009b) and Triaud et al. (2010) within error bars (1σ uncertainties).

We improve the ephemerides of WASP-4b, WASP-5b, and WASP-6b and obtain a better constrained mid-transit time for WASP-29b. Our ephemeris for WASP-19b is of similar precision to that reported by Hellier et al. (2011). Our estimates of the mid-transit times for WASP-29b and WASP-31b and those obtained by Hellier et al. (2010) and Anderson et al. (2011), respectively, are of comparable precision.

Having a long time span between our observations and the previous published mid-transit times, we update and refine the ephemerides for the six WASP systems we observed and analyzed. Our results are thus useful for planning future observations. In addition, they are consistent with previously published parameter values and as such serve to confirm the properties of these systems.

The authors thank Andrés Jordán for providing support for the observations at CTIO, and the anonymous referee who provided helpful comments that improved the manuscript. We also thank C. Hellier for the ESO NTT/EFOSC light curve of WASP-19. D.D. is supported by an FQRNT scholarship and an IPAC Visiting Graduate fellowship. M.R. acknowledges support from ALMA-CONICYT projects 31090015 and 31080021. The Center for Exoplanets and Habitable Worlds is supported by the Pennsylvania State University, the Eberly College of Science, and the Pennsylvania Space Grant Consortium.

REFERENCES

Agol, E., Steffen, J., Sari, R., & Clarkson, W. 2005, MNRAS, 359, 567
Anderson, D. R., Collier Cameron, A., Hellier, C., et al. 2011, A&A, 531, A60
Anderson, D. R., Gillon, M., Hellier, C., et al. 2008, MNRAS, 387, L4
Bakos, G. A., Noyes, R. W., Kovács, G., et al. 2004, PASP, 116, 266
Batygin, K., & Stevenson, D. J. 2010, ApJ, 715, L238
Bodenheimer, P., Lin, D. N. C., & Mardling, R. A. 2001, ApJ, 548, 466
Borucki, W. J., Koch, D. G., Basri, G., et al. 2011, ApJ, 728, 117
Burrows, A., Hubeny, I., Budaj, J., & Hubbard, W. B. 2007, ApJ, 661, 502
Carter, J. A., & Winn, J. N. 2009, ApJ, 704, 51
Charbonneau, D., Brown, T. M., Latham, D. W., & Mayor, M. 2000, ApJ, 529, L45
Claret, A. 2000, A&A, 363, 1081
Eastman, J., Siverd, R., & Gaudi, B. S. 2010, PASP, 122, 935
Everett, M. E., & Howell, S. B. 2001, PASP, 113, 1428
Fukui, A., Narita, N., Tristram, P. J., et al. 2011, PASJ, 63, 287
Gazak, J. Z., Johnson, J. A., Tonry, J., et al. 2011, arXiv:1102.1036
Gillon, M., Anderson, D. R., Triaud, A. H. M. J., et al. 2009a, A&A, 501, 785
Gillon, M., Smalley, B., Hebb, L., et al. 2009b, A&A, 496, 259
Hebb, L., Collier-Cameron, A., Triaud, A. H. M. J., et al. 2010, ApJ, 708, 224
Hellier, C., Anderson, D. R., Collier Cameron, A., et al. 2010, ApJ, 732, L60
Hellier, C., Anderson, D. R., Collier-Cameron, A., et al. 2011, ApJ, 730, L31
Holman, M. J., Winn, J. N., Latham, D. W., et al. 2006, ApJ, 652, 1715
Kane, S. R., Mahadevan, S., von Braun, K., Laughlin, G., & Ciardi, D. R. 2009, PASP, 121, 1386
Mandel, K., & Agol, E. 2002, ApJ, 580, L171
McCullough, P. R., Stys, J. E., Valenti, J. A., et al. 2005, PASP, 117, 783
Miller, N., Fortney, J. J., & Jackson, B. 2009, ApJ, 702, 1413
O'Donovan, F. T., Charbonneau, D., Mandushev, G., et al. 2006, ApJ, 651, L61
Pollacco, D. L., Skillen, I., Collier Cameron, A., et al. 2006, PASP, 118, 1407
Sanchis-Ojeda, R., Winn, J. N., Holman, M. J., et al. 2011, ApJ, 733, 127
Seager, S., & Mallén-Ornelas, G. 2003, ApJ, 585, 1038
Southworth, J., Hinse, T. C., Burgdorf, M. J., et al. 2009a, MNRAS, 399, 287
Southworth, J., Hinse, T. C., Jørgensen, U. G., et al. 2009b, MNRAS, 396, 1023
Southworth, J., Wheatley, P. J., & Sams, G. 2007, MNRAS, 379, L11
Triaud, A. H. M. J., Collier Cameron, A., Queloz, D., et al. 2010, A&A, 524, A25
von Braun, K., Abajian, M., Ali, B., et al. 2009, in IAU Symp. 253, Transiting Planets, ed. F. Pont, D. Sasselov, & M. Holman (Cambridge: Cambridge Univ. Press), 478
Wilson, D. M., Gillon, M., Hellier, C., et al. 2008, ApJ, 675, L113
Winn, J. N. 2010, arXiv:1001.2010
Winn, J. N., Holman, M. J., Carter, J. A., et al. 2009, AJ, 137, 3826